Evidence for the Fourfold-Valley Confinement Electron Piezo-Effective-Mass Coefficient in Inversion Layers of ⟨110⟩ Uniaxial-Tensile-Strained (001) nMOSFETs

Ming-Jer Chen, *Senior Member, IEEE*, and Wei-Han Lee, *Student Member, IEEE*

***Abstract*—We have recently experimentally extracted the piezo-effective-mass coefficients of 2-D electrons via the gate tunneling current of (001) n-channel metal–oxide–semiconductor field-effect transistors under ⟨110⟩ uniaxial *compressive* stress. The results pointed to the existence of a piezo-effective-mass coefficient around the fourfold conduction-band valley in the out-of-plane (quantum confinement) direction. To strengthen this further, here, we provide extra evidence. First, explicit guidelines are drawn to distinguish all the piezo-effective-mass coefficients. Then, a self-consistent strain quantum simulation is executed to fit literature data of *both* the mobility enhancement and gate current suppression in the uniaxial *tensile* stress situation. It is found that neglecting the fourfold-valley out-of-plane piezo-effective-mass coefficient, as in existing band structure calculations, only leads to a poor fitting.**

***Index Terms*—Band structure, effective mass, mechanical stress, metal–oxide–semiconductor field-effect transistors (MOSFETs), mobility, model, simulation, strain, tunneling.**

I. Introduction

ENHANCED mobility for 2-D electrons in the inversion layers of strained n-channel MOSFETs (nMOSFETs) can be microscopically elucidated upon two fundamentally distinct origins: one for the valley shift in energy [1] in terms of the deformation potential constants [2]–[4] and the other for the electron effective mass variation in a warping band structure [5], [6]. To deal with the latter, one can introduce a piezo-effective-mass coefficient π_m in a low-stress limit, according to cyclotron resonance experiments on strained n-type silicon materials [5], as follows:

$$m(\sigma) = m(0) + \pi_m \sigma \tag{1}$$

where σ is the applied mechanical stress. Corresponding π_m in a 2-D electron gas case was currently determined by a band structure calculation [7]–[10]. Mobility-based assessment of π_m was also performed [11]. However, in these methods [7]–[11], the role of the fourfold-valley Δ_4 out-of-plane π_m was overlooked. On the other hand, we recently conducted [12] a fitting of strain-altered gate electron tunneling current on (001) nMOSFETs undergoing an externally applied ⟨110⟩ compressive stress [13] and a process-induced ⟨110⟩ compressive stress [14]. This led to an argument [12] that the Δ_4 out-of-plane π_m should not be absent.

The aim of this letter is twofold: 1) to provide extra evidence in the tensile stress case; and 2) to raise concern on the current band structure calculation methods [7]–[10].

II. Guidelines and Simulators

The aforementioned study [12] revealed that, for twofold Δ_2 valleys, the confinement $\pi_{m,z\Delta 2} \approx 0$, and the 2-D density-of-states (DOS) $\pi_{m,d\Delta 2} \approx -0.017$–$-0.03$ m_0/GPa; and for Δ_4 valleys, $\pi_{m,z\Delta 4} \approx 0.03$–$0.07$ m_0/GPa and 2-D DOS $\pi_{m,d\Delta 4} \approx 0$. Apparently, a zero $\pi_{m,d\Delta 4}$ dictates that the longitudinal $\pi_{m,l\Delta 4} = 0$ and transverse $\pi_{m,t\Delta 4} = 0$, and a negative $\pi_{m,d\Delta 2}$ means that at least one of $\pi_{m,t\Delta 2\parallel}$ and $\pi_{m,t\Delta 2\perp}$ is negative and that its magnitude is larger than another having a positive value see [12, eq. 11]. These coefficients $\pi_{m,t\Delta 2\parallel}$ and $\pi_{m,t\Delta 2\perp}$ correspond to the in-plane longitudinal effective mass $m_{t,\Delta 2\parallel}$ and transverse effective mass $m_{t,\Delta 2\perp}$ of Δ_2, respectively, as shown in Fig. 1. Considering the nature of the warping band under ⟨110⟩ uniaxial stress [6], [7], we have $\pi_{m,t\Delta 2\parallel} < 0$ and $\pi_{m,t\Delta 2\perp} > 0$, but the corresponding magnitude values must be constrained by satisfying the resulting $\pi_{m,d\Delta 2}$ that lies between -0.017 and -0.03 m_0/GPa.

Thus, explicit guidelines can be created as follows. For Δ_4 valleys, $\pi_{m,d\Delta 4} = 0$, $\pi_{m,l\Delta 4} = 0$, $\pi_{m,t\Delta 4} = 0$, and $\pi_{m,z\Delta 4}$ ranges from 0.03 to 0.07 m_0/GPa; and for Δ_2 valleys, $\pi_{m,z\Delta 2} = 0$, $\pi_{m,t\Delta 2\parallel} < 0$, $\pi_{m,t\Delta 2\perp} > 0$, and $\pi_{m,d\Delta 2}$ of -0.017–-0.03 m_0/GPa. Obviously, only three coefficients, $\pi_{m,z\Delta 4}$, $\pi_{m,t\Delta 2\parallel}$, and $\pi_{m,t\Delta 2\perp}$ are needed in the subsequent simulation, with other π_m's kept at zero.

To quantify the strain-altered electron mobility and gate tunneling current, the following numerical solvers and/or simulators, as readily available in the previous studies [12], [15], [16], have been integrated: 1) a self-consistent solver of Schrödinger and Poisson's equations [15], [16]; 2) a gate electron tunneling current simulator [12]; and 3) an electron mobility simulator

Manuscript received February 2, 2012; accepted March 1, 2012. Date of publication April 18, 2012; date of current version May 18, 2012. This work was supported by the National Science Council of Taiwan under Contract NSC 100-2221-E-009-017-MY3. The review of this letter was arranged by Editor C. P. Yue.

The authors are with the Department of Electronics Engineering and Institute of Electronics, National Chiao Tung University, Hsinchu 300, Taiwan (e-mail: chenmj@faculty.nctu.edu.tw).

Color versions of one or more of the figures in this letter are available online at http://ieeexplore.ieee.org.

Digital Object Identifier 10.1109/LED.2012.2190579

π_m (m_0/GPa)	Condition 1	Condition 2	Condition 3	Condition 4
$\pi_{m,z\Delta4}$	0	0.03	0.05	0.07
$\pi_{m,t\Delta2//}$	-0.02	-0.04	-0.05	-0.055
$\pi_{m,t\Delta2\perp}$	0.02	0.02	0.01	0
Other π_m	0	0	0	0

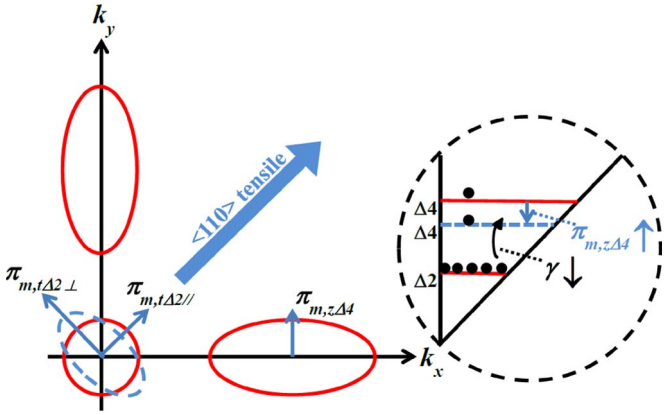

Fig. 1. Schematic diagram of one Δ_2 valley and two Δ_4 valleys in k_x-k_y plane. The channel length direction is along the $\langle 110\rangle$ uniaxial tensile stress direction on the (001) substrate. The dashed line around the Δ_2 valley in terms of the longitudinal $\pi_{m,t\Delta2\|}$ and transverse $\pi_{m,t\Delta2\perp}$, as well as the $\Delta_4\pi_{m,z\Delta4}$, shows the effect of stress. One of the two insets is for the π_m values used for simulation in Figs. 3 and 4; and the other for the demonstration of the effect of $\pi_{m,z\Delta4}$.

[16] accounting for both phonon scattering and surface roughness scattering. The strain Hamiltonian [17] has also been incorporated into Schrödinger and Poisson's equations solvers [15], [16]. Such a sophisticated combination constitutes a self-consistent strain quantum simulation tool. Note that, relative to the triangular potential approach in [12], the presented self-consistent version in this letter can provide accurate wave functions that are needed in the mobility calculation.

III. Results and Discussion

Mobility enhancement data [7] are plotted in Fig. 2 versus vertical effective field. The detailed information [7] is that the channel length direction is along the $\langle 110\rangle$ direction on (001) nMOSFETs; two in-plane uniaxial tensile stresses, i.e., $\sigma_\|$ and $\sigma_\perp$, are externally applied in the $\langle 110\rangle$ and $\langle -110\rangle$ directions, respectively; and phonon-scattering-limited mobility enhancement is simulated with zero π_m, as together plotted. Simulated mobility enhancement in this letter with zero π_m is shown for validation. The nonstress effective mass values [i.e., $m(0)$ in (1)] used in simulation were the same as the previous work (see [12, Table I]). Good agreement with that of [7] is evident, which is valid for a wide range of substrate doping concentrations. Additional simulation results by varying $\pi_{m,z\Delta4}$ reveal that an increase in $\pi_{m,z\Delta4}$ will degrade mobility.

Interestingly, for the case of $\pi_{m,z\Delta4}=0$, $\sigma_\|$ and $\sigma_\perp$ mobility data can be fitted well by separately adjusting $\pi_{m,t\Delta2\|}$ and $\pi_{m,t\Delta2\perp}$ to -0.02 and 0.02 m_0/GPa, which are close to those of the citation [7]. Such a fitting is repeated for other values of $\pi_{m,z\Delta4}$. The results are plotted in Fig. 3. Corresponding π_m's are given in Fig. 1 in terms of four different conditions. Clearly,

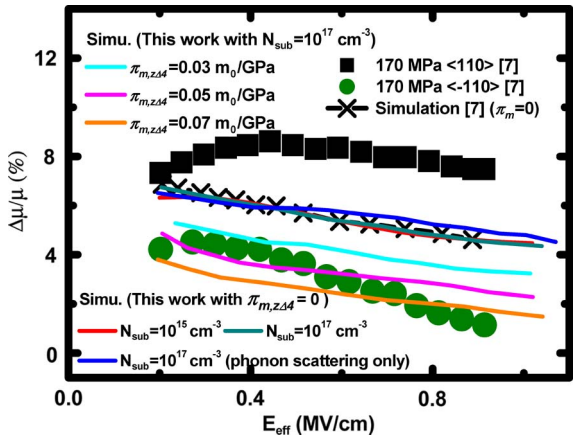

Fig. 2. Comparison of (cross symbols) simulated mobility enhancement due to $\langle 110\rangle$ 170 MPa with zero π_m [7] and those (lines) obtained in this letter under different simulation conditions (substrate doping concentration $N_{\rm sub}$ of 10^{15} and 10^{17} cm^{-3} and $N_{\rm sub}$ of 10^{17} cm^{-3} without surface roughness scattering), all plotted versus vertical effective field. The (lines) simulated mobility enhancement values with and without surface roughness scattering are comparable of each other, indicating that phonon scattering dominates. Other simulation lines are produced to highlight the impact of the $\pi_{m,z\Delta4}$ alone.(Squares and circles) Data [7] are together plotted for comparison.

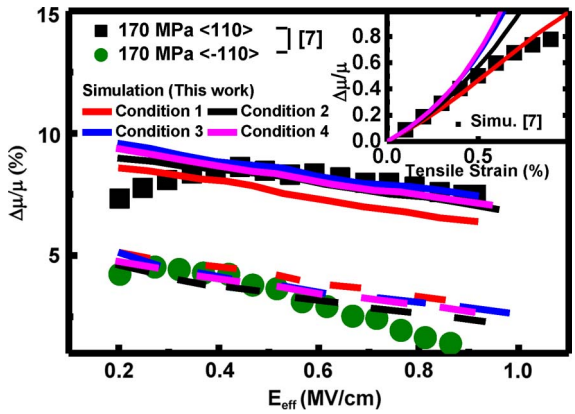

Fig. 3. Comparison of (symbols) mobility enhancement data [7] under $\langle 110\rangle$ and $\langle -110\rangle$ 170-MPa tensile stress with (lines) the simulated ones for four different conditions in Fig. 1, which are plotted versus vertical effective field. The substrate doping concentration of 10^{17} cm^{-3} is used in this letter. The inset shows the comparison of simulated mobility enhancement versus tensile strain with the published simulation values [7].

both $\pi_{m,t\Delta2\|}$ and $\pi_{m,t\Delta2\perp}$ are coupled with the $\pi_{m,z\Delta4}$: $\pi_{m,t\Delta2\|}$ increases negatively with $\pi_{m,z\Delta4}$, whereas $\pi_{m,t\Delta2\perp}$ exhibits a decreasing trend. The extracted values of π_m are further used to calculate the gate tunneling current change under uniaxial tensile stress. The results are shown in Fig. 4, along with the literature data [18], [19] for comparison. It can be seen that the higher the $\pi_{m,z\Delta4}$, the less the deviation it will produce. Meanwhile, good agreement with mobility data holds, as in Fig. 3.

Therefore, the coefficient $\pi_{m,z\Delta4}$ plays a vital role. To highlight this, we show in Fig. 1 that an increase in $\pi_{m,z\Delta4}$ increases the Δ_4 quantization effective mass under tensile stress, which will in turn render the Δ_4 level lowered. As a result of the valley repopulation, more electrons jump from Δ_2 to Δ_4. This reflects a decrease in the Δ_2 valley occupancy. Thus, there are two effects caused solely by varying $\pi_{m,z\Delta4}$: The gate tunneling current is increased, and the mobility is degraded. The

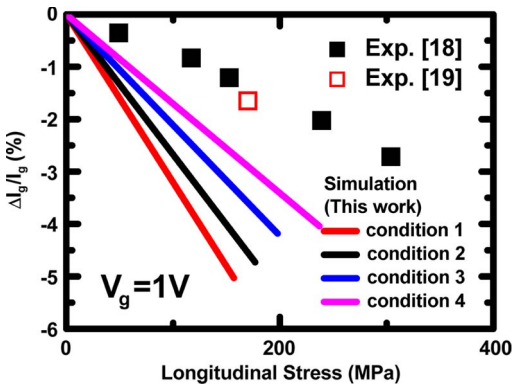

Fig. 4. Comparison of (symbols) gate current change data [18], [19] at $V_g = 1$ V with (lines) those simulated under four different conditions in Fig. 1, which are plotted versus $\langle 110 \rangle$ tensile stress magnitude. The gate oxide thickness and substrate doping concentration used in simulation are 1.3 nm and 5×10^{17} cm^{-3}, as in [18].

detailed interpretations, as already presented in the opposite case (compressive) [12], can be applied to the former. As to the latter, the following formula may be useful:

$$\mu = \frac{q\tau_{\Delta 2}}{m_{c,\Delta 2}}\gamma + \frac{q\tau_{\Delta 4}}{m_{c,\Delta 4}}(1-\gamma) \tag{2}$$

where $\tau_{\Delta 2}$ and $\tau_{\Delta 4}$ represent the mean scattering time of Δ_2 and Δ_4 valleys, respectively; γ represents the Δ_2 valley occupancy; and $m_{c,\Delta 2}$ and $m_{c,\Delta 4}$ are the conductivity effective mass of Δ_2 and Δ_4, respectively. Here, $m_{c,\Delta 2} = m_{t,\Delta 2\|}$ for $\langle 110 \rangle$ stress or $m_{t,\Delta 2\perp}$ for $\langle -110 \rangle$ stress, and $m_{c,\Delta 4} = 2(m_{t,\Delta 4} m_{l,\Delta 4})/(m_{t,\Delta 4} + m_{l,\Delta 4})$ [20]. A decrease in γ favors the second term of (2) featuring a higher $m_{c,\Delta 4}$, which will in turn degrade the overall mobility.

Further simulation was done at higher tensile stress. The comparison of simulated mobility enhancement with the published ones [7] is inserted in Fig. 3, which is plotted versus tensile strain of up to 1%. Fairly good agreement is reached for Condition 1 whose π_m's are close to [7] (see [12, Table II]). This validates the presented self-consistent strain quantum simulation. For other conditions, mobility enhancement strongly increases, particularly in the higher tensile strain region. However, there is one of the fundamental limits that must be kept in mind: π_m in (1) essentially works in low-stress situations. Indeed, such a low tensile strain region can be located ($< 0.2\%$), where the simulated mobility enhancement coincides with that of [7], regardless of the simulation conditions used. Straightforwardly, we want to stress that the current band structure calculation methods [7]–[10] did not explicitly address the significance of the Δ_4 out-of-plane π_m. Thus, in the area of band structure calculations, a further investigation is needed in this direction.

IV. Conclusion

Explicit guidelines have been drawn for all the piezo-effective-mass coefficients: 1) for Δ_4 valleys, $\pi_{m,d\Delta 4} = 0$, $\pi_{m,l\Delta 4} = 0$, $\pi_{m,t\Delta 4} = 0$, and $\pi_{m,z\Delta 4}$ of 0.03–0.07 m_0/GPa; and 2) for Δ_2 valleys, $\pi_{m,z\Delta 2} = 0$, $\pi_{m,t\Delta 2\|} < 0$, $\pi_{m,t\Delta 2\perp} > 0$, and $\pi_{m,d\Delta 2}$ of -0.017 to -0.03 m_0/GPa. The self-consistent strain quantum simulation has been carried out while fitting both the enhanced mobility and suppressed gate current data under $\langle 110 \rangle$ uniaxial tensile stress. The results have corroborated the fourfold-valley out-of-plane $\pi_{m,z\Delta 4}$ and have suggested the required reexamination of the current band structure calculations.

References

[1] M. V. Fischetti and S. E. Laux, "Band structure, deformation potentials, and carrier mobility in strained Si, Ge, and SiGe alloys," *J. Appl. Phys.*, vol. 80, no. 4, pp. 2234–2252, Aug. 1996.

[2] C. Herring and E. Vogt, "Transport and deformation-potential theory for many-valley semiconductors with anisotropic scattering," *Phys. Rev.*, vol. 101, no. 3, pp. 944–961, Feb. 1956.

[3] I. Balslev, "Influence of uniaxial stress on the indirect absorption edge in silicon and germanium," *Phys. Rev.*, vol. 143, no. 2, pp. 636–647, Mar. 1966.

[4] C. G. Van de Walle and R. M. Martin, "Theoretical calculations of heterojunction discontinuities in the Si/Ge system," *Phys. Rev. B*, vol. 34, no. 8, pp. 5621–5634, Oct. 1986.

[5] J. C. Hensel, H. Hasegawa, and M. Nakayama, "Cyclotron resonance in uniaxially stressed silicon. II. Nature of the covalent bond," *Phys. Rev.*, vol. 138, no. 1A, pp. A225–A238, Apr. 1965.

[6] Y. Kanda and K. Suzuki, "Origin of the shear piezoresistance coefficient π_{44} of n-type silicon," *Phys. Rev. B*, vol. 43, no. 8, pp. 6754–6756, Mar. 1991.

[7] K. Uchida, T. Krishnamohan, K. C. Saraswat, and Y. Nishi, "Physical mechanisms of electron mobility enhancement in uniaxial stressed MOSFETs and impact of uniaxial stress engineering in ballistic regime," in *IEDM Tech. Dig.*, 2005, pp. 129–132.

[8] S. Dhar, E. Ungersböck, H. Kosina, T. Grasser, and S. Selberherr, "Electron mobility model for $\langle 110 \rangle$ stressed silicon including strain-dependent mass," *IEEE Trans. Nanotechnol.*, vol. 6, no. 1, pp. 97–100, Jan. 2007.

[9] E. Ungersboeck, S. Dhar, G. Karlowatz, V. Sverdlov, H. Kosina, and S. Selberherr, "The effect of general strain on the band structure and electron mobility of silicon," *IEEE Trans. Electron Devices*, vol. 54, no. 9, pp. 2183–2190, Sep. 2007.

[10] V. Sverdlov, *Strain-Induced Effects in Advanced MOSFETs*. Berlin, Germany: Springer-Verlag, 2011.

[11] F. Rochette, M. Cassé, M. Mouis, G. Reimbold, D. Blachier, C. Leroux, B. Guillaumot, and F. Boulanger, "Experimental evidence and extraction of the electron mass variation in [110] uniaxially strained MOSFETs," *Solid State Electron.*, vol. 51, no. 11/12, pp. 1458–1465, Nov./Dec. 2007.

[12] W. H. Lee and M. J. Chen, "Gate direct tunneling current in uniaxially compressed strained nMOSFETs: A sensitive measure of electron piezo effective mass," *IEEE Trans. Electron Devices*, vol. 58, no. 1, pp. 39–45, Jan. 2011.

[13] J. S. Lim, X. Yang, T. Nishida, and S. E. Thompson, "Measurement of conduction band deformation potential constants using gate direct tunneling current in n-type metal oxide semiconductor field effect transistors under mechanical stress," *Appl. Phys. Lett.*, vol. 89, no. 7, pp. 073509-1–073509-3, Aug. 2006.

[14] C. Y. Hsieh and M. J. Chen, "Measurement of channel stress using gate direct tunneling current in uniaxially stressed nMOSFETs," *IEEE Electron Device Lett.*, vol. 28, no. 9, pp. 818–820, Sep. 2007.

[15] M. J. Chen, C. C. Lee, and K. H. Cheng, "Hole effective masses as a booster of self-consistent six-band $k \cdot p$ simulation in inversion layers of pMOSFETs," *IEEE Trans. Electron Devices*, vol. 58, no. 4, pp. 931–937, Apr. 2011.

[16] M. J. Chen, S. C. Chang, S. J. Kuang, C. C. Lee, W. H. Lee, K. H. Cheng, and Y. H. Zhan, "Temperature-dependent remote-Coulomb-limited electron mobility in n^+-polysilicon ultrathin gate oxide nMOSFETs," *IEEE Trans. Electron Devices*, vol. 58, no. 4, pp. 1038–1044, Apr. 2011.

[17] Y. Sun, S. E. Thompson, and T. Nishida, "Physics of strain effects in semiconductors and metal-oxide-semiconductor field-effect transistors," *J. Appl. Phys.*, vol. 101, no. 10, pp. 104 503-1–104 503-22, May 2007.

[18] X. Yang, Y. Choi, T. Nishida, and S. E. Thompson, "Gate direct tunneling currents in uniaxial stressed MOSFETs," in *Proc. IEDST*, 2007, pp. 149–152.

[19] W. Zhao, A. Seabaugh, V. Adams, D. Jovanovic, and B. Winstead, "Opposing dependence of the electron and hole gate currents in SOI MOSFETs under uniaxial strain," *IEEE Electron Device Lett.*, vol. 26, no. 6, pp. 410–412, Jun. 2005.

[20] F. Stern, "Self-consistent results for n-type Si inversion layers," *Phys. Rev. B*, vol. 5, no. 12, pp. 4891–4899, Jun. 1972.